Update of E-09-019 to the Jefferson Lab Program Advisory Committee (PAC35)

Precision Measurement of the Neutron Magnetic Form Factor up to Q^2=13.5 (GeV/c)^2 by the Ratio Method

B. Quinn, B. Wojtsekhowski(contact), R. Gilman and E-09-019 collaboration

1 Introduction

The neutron magnetic form factor is almost as large as that of the proton and should be easily measurable. However, the results from single arm experiments, possible with pulsed accelerators, have large systematic uncertainties. Single arm (e,e') measurements of G_M^n were performed for Q^2 up to 10 (GeV/c)^2 [1] with an uncertainty of 10-25%. Fifty years ago Durand [2] suggested a technique for precision G_M^n/G_M^p measurement by detecting the scattered electron and recoiling nucleon in coincidence and measuring a ratio of the cross sections for the two quasi-elastic processes, D(e,e'n) and D(e,e'p). This became practical with the advent of CW electron accelerators. Several measurements have been performed with the ratio method, including recent results from JLab up to Q^2 of 4.5 (GeV/c)^2 [3], with a 4 GeV electron beam. Advancing to higher momentum transfer is very important but requires a higher beam energy and much higher luminosity.

We propose to use the Ratio Method to accurately determine the magnetic elastic form factor of the neutron at seven values of Q^2, greatly extending the kinematic range over which high precision measurements are available. We will make measurements centered at $Q^2 = 3.5$, 4.5, 6.5, 8.5, 10., 12., and 13.5 (GeV/c)^2. Using pieces of the Super BigBite apparatus, we will be able to measure G_M^n in a 31-day run with total accuracy better than 2-3% as shown in Fig. 1. Two points at still higher Q^2 were not approved by PAC34. Those points, with the experimental improvements discussed here, have been submitted as a separate proposal to this PAC.

A significant improvement in the design of the experiment has been made possible because of progress on the design of the Hadron Calorimeter (HCal) for the Super BigBite Spectrometer (SBS) to be built for Hall A. The implications of this are discussed in Section 4.

A CLAS12 experiment [4], E12-07-104, will also make measurements over a similar kinematic range. In order to allow more direct comparison with that experiment, the calculations in our original proposal were based upon the scaled dipole form factors, as used in that proposal. In this update, we change to a more conservative parametrization for the form factors used in estimating rates and background contamination. We use a recent parameterization by Bodek which is [5] based on that of Kelly [6] but incorporates high-Q^2 behavior consistent with quark-hadron duality predictions. As shown in Fig. 1, the predicted value of G_M^n is significantly smaller than the prediction of the dipole. It is also smaller than the prediction of Kelly, and significantly smaller than the prediction of Alberico [7] (used in more recent CLAS12 rate estimates) giving a more conservative representation of the experimental challenges.

Fig. 1 shows the updated error estimates based on simulations done with HCal and the Bodek form factors.

2 Scientific Motivation for the Measurement

The motivation for all four nucleon form-factor experiments was discussed extensively in the update for the GEp(5) experiment [8]. Here we present a few considerations related particularly to the G_M^n form factor.

Form factor measurements provide information about the distribution of a hadron's characteristic properties amongst its QCD constituents. In the domain 1-6 GeV^2, the G_E^p/G_M^p ratio exhibits a clear trend and G_E^p suggesting it will pass through zero. This is a natural domain in which to seek precision information on G_M^n/G_M^p. A calculation of the evolution of form factors at $Q^2 > 1$ GeV^2 requires a Poincaré-covariant approach [9]. Dyson-Schwinger predictions of the ratio G_M^n/G_M^p can now be made using a Poincaré covariant framework, which incorporates essential elements of QCD such as the momentum-dependent dressing of the propagators of QCD's elementary excitations, and so confinement and dynamical chiral symmetry breaking [10]. Such predictions relate data to the connection between confinement and dynamical chiral symmetry breaking (DCSB), the most important mass generating mechanism for matter in the universe, the Higgs mechanism being irrelevant to light-quarks.

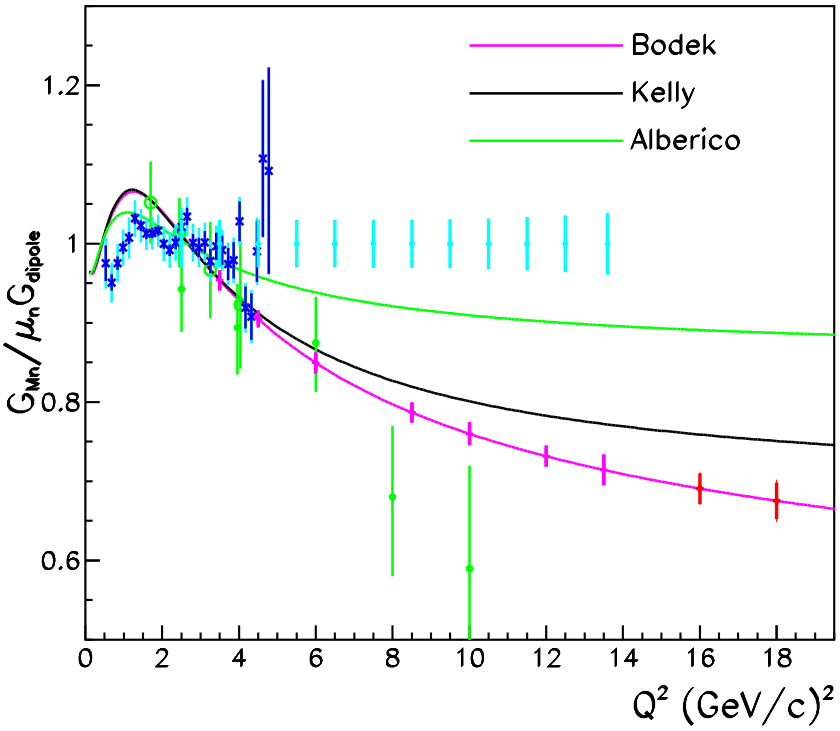

Figure 1: Existing data on G_M^n in the Q^2 range of this measurement are plotted as ratio to scaled dipole approximation. Blue points are from CLAS e5 run [3, 17]. Dark blue lines show the statistical error while light blue extensions show the quadrature sum of statistical and systematic errors. Solid green circle [1] and hollow green circle [16] points are from SLAC. Magenta points (plotted at value used in simulations) show projected size of error bars for points approved for E-09-019. Red points show the projected errors for the measurements proposed separately (E-10-005) to this PAC. Error bars include projected statistical and systematic errors of the proposed experiment and also estimated errors on G_E^n and on the proton elastic cross section. Solid light-blue circles with error bars (arbitrarily plotted at 1.0) indicate the position and projected total errors [15] of the CLAS12 experiment. Three recent parameterizations (see text) are shown for comparison as solid lines: magenta for Bodek [5], black for Kelly [6] and green for Alberico [7].

The measurements also relate to the distribution over constituents within the nucleon of: mass, momentum, orbital angular momentum, etc. This constitutes a QCD map of nucleons. New data on G_M^n /G_M^p will enable better-constrained models, building insight into the mass and current operators in QCD, helping to constrain predictions: of elastic and transition form factors; of parton distribution functions, both spin-independent and spin-dependent; and of the spectrum of nucleon resonances. It will also enable progress toward understanding the relationship between parton properties on the light-front and the rest frame structure of hadrons. This is an open problem because, e.g., DCSB, an established keystone of low-energy QCD and the origin of constituent-quark masses, has not been realized in the light-front formulation. In the absence of neutron data, theory will continue to be biased by proton properties.

Assuming strange-quark contributions are negligible, the data on G_M^n combined with three other form factor experiments will allow separation of the form factors into individual contributions from the u($\bar{u}$) and d($\bar{d}$) quarks. This will, for example, allow separate analysis of the quark form factors $F_{1(2)}^{u(d)}$ as illustrated for F_1^d/F_1^u in Figure 2.

Not only will the proposed measurement of G_M^n allow us to perform iso-spin analysis of the nucleon form factor at very large momentum transfer, it will also allow us to map out the neutron transverse charge density at very short distance scale to the level of 0.05 fm.

3 The Concept of the Experiment

Experiment E12-09-019 will use 4.4 to 11 GeV electron beam energies on a liquid deuterium target. (A hydrogen target will be used for calibration of the detector system.) Selection of the quasi-elastic process is based on the angular correlation between the momentum transfer and the momentum of the recoiling nucleon. Inelastic events related to meson production which have much wider angular correlation will be suppressed by a tight cut on this angular correlation.

The quasi-elastic processes D(e,e'p) and D(e,e'n) will be measured simultaneously. The ratio of coincidence rates allows determination of the ratio of magnetic form factors after minimal corrections due to the electric form factors, nuclear effects and two-photon effects.

The high energy of the recoiling nucleons insures a high detection efficiency in the segmented hadron calorimeter. The

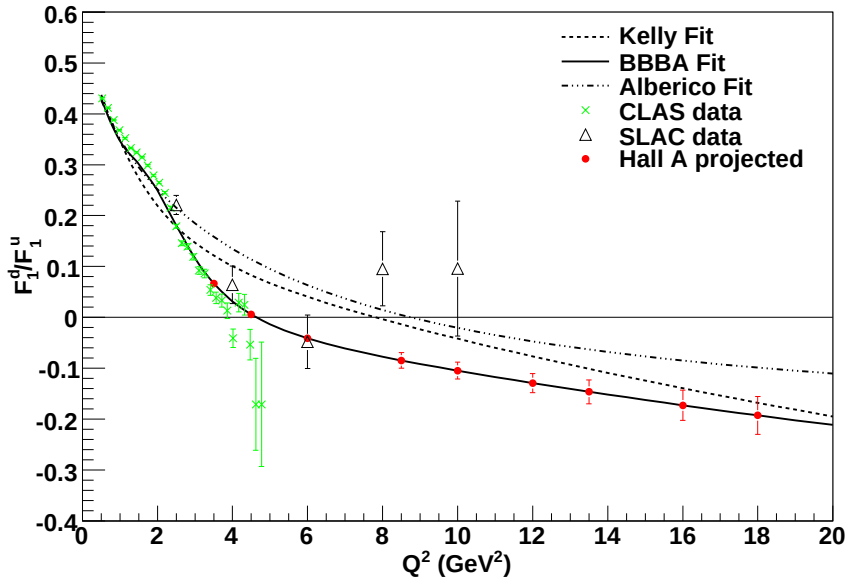

Figure 2: The ratio of the proton quark form factors F_1^d and F_1^u. The points shown are the same as in Fig. 1.

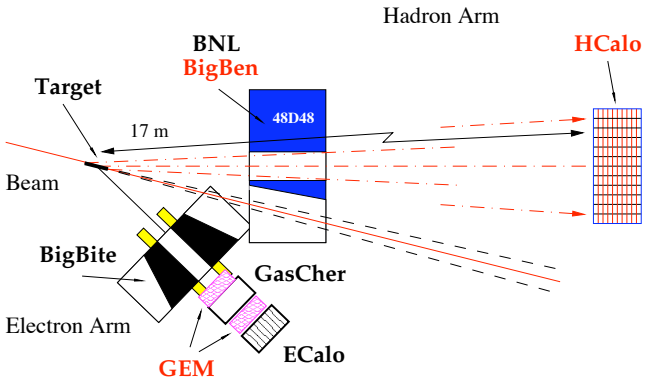

Figure 3: The layout of the E12-09-019 experiment with the Super BigBite apparatus.

two arms of the experiment, the electron arm and the nucleon arm, are separate, allowing calibration to be performed with different magnetic field settings. The layout of the experimental equipment is shown in Fig. 3

All detectors in this experiment are parts of the GEp(5) system [11, 12] or are already constructed and have become standard in Hall A.

The scattered electron will be detected in the BigBite spectrometer originally constructed for GEn(1) [13]. The tracking planes of BigBite will be replaced with GEM detectors allowing efficient operation at much higher luminosity.

The recoiling nucleons will be detected in a hadron calorimeter, located up to 17 m from the target, behind a large-acceptance dipole magnet of the Super BigBite. The individual calorimeter blocks of the hadron calorimeter will be similar to ones used [14] in the COMPASS experiment at CERN.

The dipole magnet of SBS is available from the fixed-target AGS program at BNL. The dipole will bend elastically scattered recoiling protons by $\approx$6 degrees upwards. A cutout in the SBS magnet allows for the use of forward angles to 12-14° where the recoil protons need to be detected with a large solid angle.

Table 1: Kinematics and setup of proposed measurements Entrance of BigBen is 1.6 m from target except at highest Q^2 points where it is 1.8 m for $\theta_N = 13.3^\circ$ and 2.5 m for $\theta_N = 9.8^\circ$.

Q^2 (GeV/c)^2	E_{beam} (GeV)	θ_e	θ_N	E' (GeV)	P_N (GeV/c)	R_{HCal} (m)	$\int B\,dl$ (T-m)	Equiv. p_{Kick} (MeV/c)	$\mathcal{L}(\times 10^{38}/A$ (/cm^2/s)
3.5	4.4	32.5°	31.1°	2.5	2.6	6.2	1.4	270	0.7
4.5	4.4	41.9°	24.7°	2.0	3.2	6.2	1.7	350	1.4
6.	4.4	64.3°	15.6°	1.2	4.0	11	0.7	250	2.8
8.5	6.6	46.5°	16.2°	2.1	5.4	11	1.2	250	2.8
10.	8.8	33.3°	17.9°	3.5	6.2	13	1.3	340	1.4
12.	8.8	44.2°	13.3°	2.4	7.3	14	1.2	350	2.8
13.5	8.8	58.5°	9.8°	1.6	8.1	17	0.9	330	2.8

4 Update of Experiment

The use of HCal in place of BigHAND, for the detection of coincident nucleons presents three significant experimental benefits:

- Higher threshold
- Higher efficiency
- Improved spatial resolution

The advantages of each of these are discussed below.

4.1 Higher threshold

The higher threshold is made possible by the structure of HCal, whose 15 × 15 cm^2 modules are composed of 40 alternating layers of iron and scintillator. The large energy-deposited expected for the hadronic shower of a high momentum nucleon cannot be emulated by a low energy particle. Since BigBite will be instrumented with GEM detectors, which can operate in a high-rate environment, the change to HCal greatly increases the luminosity at which data can be taken. The kinematics of the planned measurements are shown in Table 1. The luminosity was kept at the original value for the lowest Q^2 point, but it was doubled for the second Q^2 point and quadrupled for all higher Q^2 points with the exception of $Q^2 = 10$ (GeV/c)^2, which requires a small electron-scattering angle.

This increase in luminosity more than offsets the effect of the more conservative assumptions made for the nucleon form factors. The resulting higher statistics, especially for neutron coincidences, have more profound effects than simply reducing the statistical errors. They allow tighter cuts to be used to enhance the purity of the signal and reduce systematic errors. They would also permit the sub-division of our measurements into smaller Q^2 bins. Tight fiducial cuts, for example, help reduce the systematic error due to possible differences in acceptance for the two nucleon species. More importantly, tighter cuts can be made on θ_{pq} (the angle between the reconstructed $\vec{q}$ vector and the observed nucleon momentum direction) and W^2 (the squared mass of the hadronic system, calculated assuming the electron struck a nucleon at rest). Table 2 lists the cuts assumed for the simulations used in this update and the resulting inelastic contamination. The fractional contamination (defined as ratio of background events to total events within cuts) is seen to be well controlled. Subtraction of these background events increases the statistical error of the measurement. Furthermore any inaccuracy in the estimate of the contamination results in a systematic error. For the purpose of these estimates, it was assumed that the contamination could only be estimated with an accuracy of 20% of the inelastic contamination. This assumed inaccuracy in subtraction of inelastic events is a dominant contribution to the systematic errors. It should be noted that these cuts have not been pushed to the limit which simulation suggests is possible. Tighter cuts would further reduce the contamination and therefore the systematic errors, with

Table 2: Estimated fractional contamination of inelastic events in the quasi-elastic sample after W^2 and θ_{pq} cuts but *before any correction is applied*

Q^2 (GeV/c)^2	3.5	4.5	6.0	8.5	10.	12.	13.5	16.	18.
Max. θ_{pq} (deg.)	2.5	2.3	2.0	1.1	0.9	0.7	0.6	0.5	0.5
Max. W^2 (GeV^2)	1.0	1.1	1.1	1.3	1.4	1.1	1.1	1.6	2.0
Proton contamination (bkg/tot) (%)	0.5	2.1	86.4	7.8	6.3	10.5	13.8	13.5	19.9
Neutron contamination (bkg/tot) (%)	1.3	5.2	15.5	17.4	16.0	19.8	28.0	28.0	34.0

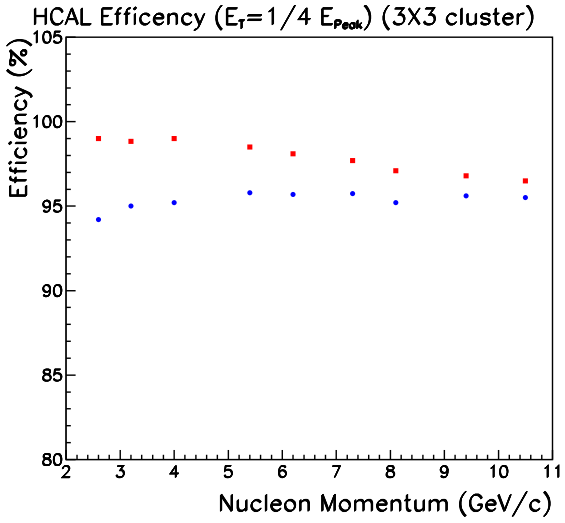

Figure 4: Efficiency for detection of neutrons (blue) and protons (red) found from Geant4 simulation [18, 19] of HCal. Each point represents one of the seven kinematic points of measurement. (Two proposed points at higher Q^2 are also shown.) For each case the threshold is taken to be one quarter of the peak energy-deposited.

an acceptable trade-off of increased statistical errors. Conservative estimates were made by restricting the fraction of the Quasi-elastic events passing the cut to be greater than 50% (43% for the two highest Q^2 points). If the actual data shows this predicted behavior, it may be advantageous to trade away statistics by tightening the cuts still further to control systematic errors. While such tight cuts might result in alarming acceptance corrections in a cross section experiment, it should be noted that the acceptance losses, which are based only upon measurements in the electron arm, are essentially identical for both nucleon species and cancel in the ratio of interest in this experiment.

4.2 Higher efficiency

The expected [18, 19] efficiency of HCal at the nucleon momenta of interest is shown in Fig. 4. The efficiencies are seen to be very high and to differ by at most 5% for the two nucleon species. While the higher efficiency has a minor effect of increasing the statistics of the measurement, it has greater effect on the control of systematic errors.

The correction for nucleon detection efficiencies would be expected to be only 5% at worst, much smaller than was true with BigHand. Even without efficiency measurements this could probably be estimated at the level of 10% of the correction, contributing 0.5% systematic error, at worst, and much less for the highest Q^2 values. The contribution to the systematic error has been very conservatively estimated at 0.5% at each point, as indicated in Table 3.

It is still prudent to check the simulations with calibration measurements but these are now expected to have less direct effect on the systematic errors. We propose to reduce the number of points at which neutron calibrations are done to two instead of three. These would be done at $Q^2 = 3.5$ and 6.0 (GeV/c)^2 (p$_N$=2.6 and 4.0 GeV/c). These measurements will serve to check (and possibly calibrate) the simulations and will allow a detailed study of the effect of threshold on efficiency.

Because HCal will be built of identical modules and the efficiency depends mostly on the distribution of material, not the PMT gain (and because the efficiency correction is less critical) it will be sufficient to illuminate a fraction of the HCal face with tagged neutrons. This permits an additional modification of the planned measurements. A High Resolution

Table 3: Estimated contributions (in percent) to systematic errors on R.

Q^2 (GeV/c)^2	3.5	4.5	6.0	8.5	10.	12.	13.5	16.	18.
proton cross-section	1.7	1.7	1.7	1.7	1.7	1.7	1.7	1.7	4.
G_E^n	1.8	1.4	0.67	0.81	2.0	1.28	0.74	.929	.42
Nuclear correction,	-	-	-	-	-	-	-	-	-
Accidentals	-	-	-	-	-	-	-	-	-
Target windows	.2	.2	.2	.2	.2	.2	.2	.2	.2
Acceptance losses	0.1	0.07	0.2	0.16	0.1	0.16	0.13	0.16	.11
Inelastic contamination	0.16	0.7	2.3	2.5	2.5	2.7	4.6	4.6	5.4
Nucleon mis-identification	1.	0.3	0.6	1.	0.3	0.3	0.3	0.3	0.3
HCal calibration	0.5	0.5	0.5	0.5	0.5	0.5	0.5	0.5	0.5
Without proton err.									
Syst. error on G_M^n/G_M^p	1.07	0.84	1.32	1.36	1.62	1.47	2.34	2.52	2.74
With proton err.									
Syst. error on G_M^n	1.37	1.19	1.57	1.6	1.83	1.70	2.49	2.66	3.39

Spectrometer (HRS) can be used in place of BigBite to measure the π^+ which tags neutron production in the p(γ,π^+)n calibration reaction. This has the advantage that the superb resolution of the HRS can more cleanly isolate the bremsstrahlung end-point and eliminate any potential contamination from p(γ,2π). Even with a 6σ cut on pion momentum to exclude the two-pion production threshold, the usable photon flux is roughly double that estimated in the proposal. Fig. 5 shows the portion of the HCAL face which would be illuminated with calibration neutrons at each of the kinematics (assuming the HCal is moved back to 17 m from the target for calibration).

4.3 Improved spatial resolution

The predicted HCal spatial resolution (in x- or y- direction) at momenta of interest, shown in Fig. 6, is superior to that of BigHAND. This has several consequences reducing systematic errors.

Spatial resolution is critical for the θ_{pq} cut which rejects inelastic contamination, the source of the dominant systematic error at high Q^2. The superior resolution permits more flexibility in the choice of HCal position. HCal can be brought closer to the target (especially at low Q^2 where the θ_{pq} distribution is wider) to allow a better match of the angular coverage for the electron and nucleon arms. In addition to increasing the useful solid angle, this has the effect of reducing acceptance corrections for loss of nucleons because of Fermi momentum (especially when appropriate fiducial cuts are applied on the electron arm). With the detector positions indicated in Table 1, the simulation indicates acceptance losses of less than 2% in each case. Since the losses are similar for neutrons and protons, the contribution to systematic errors on the ratio is reduced to negligible levels (taken in Table 3 to be 10% of the correction).

The flexibility in choice of position of HCal can be combined with a stronger magnetic 'kick' by the BigBen dipole to give a cleaner separation of neutrons and protons while still allowing the majority of the proton 'image' to remain on the face of HCal. This cleaner separation is represented in Table 1 as $p_{\rm Kick}$, the nucleon Fermi momentum which would be required to displace a nucleon to the expected position of the other species. This 'kick' is seen, in every case, to be large compared to the 200 MeV/c value discussed in the proposal, which might allow a 5% mis-identification. Even that estimate is probably high, being based on a large high-momentum tail of the deuteron wave-function and neglecting the effect of the θ_{pq} cut. Furthermore, the mis-identification can be corrected by observing the tail of the distribution in the direction opposite to that in which the other nucleon species is to be found. Table 3 reflects a generous estimate for the resulting systematic error of 1% for the cases with $p_{\rm Kick} < 300$ MeV/c and 0.3% otherwise.

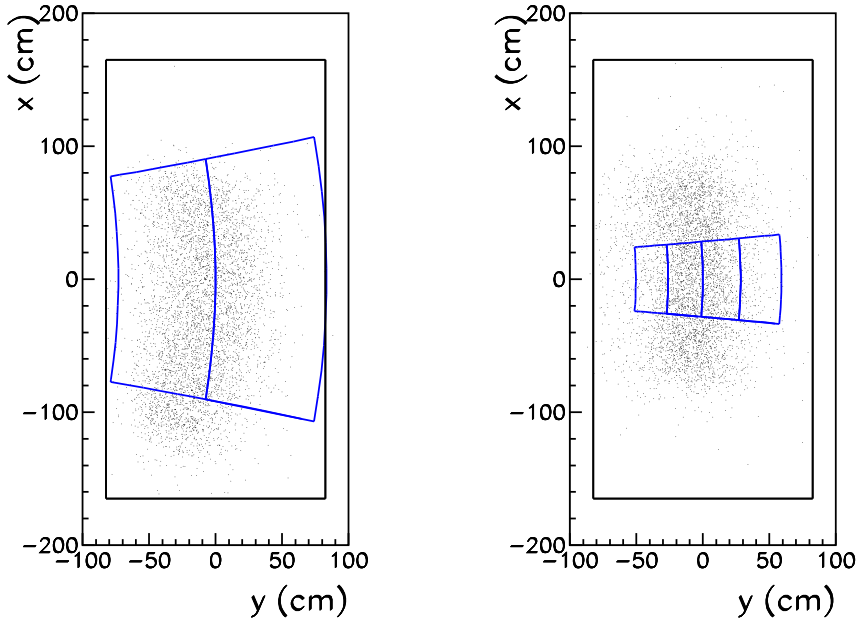

Figure 5: The region of calibration neutrons on the face of HCal is represented for the $Q^2 = 3.5$ (left) and 6.0 (GeV/c)^2 kinematics (right), but with HCal assumed to be $R_{\rm HCal}$=17 m from the target for calibration measurements. Simulated quasielastic neutrons are also shown to indicate the region of interest (at the nominal $R_{\rm HCal}$ for each of the kinematics). Each blue box represents the region which would be illuminated by tagged neutrons for a particular HRS position. Two HRS positions are shown for the lower Q^2 point and four for the higher Q^2.

5 Beam Request

The details of the beam request are shown in Table 4. A total of 31 days of beam are requested at energies of 4.4, 6.6 and 8.8 GeV. This is essentially equal to the original request, excluding the time which was originally requested for the higher Q^2 points with 11 GeV beam, which were not approved as part of this experiment.

There are some changes in the details of the beam request. An additional twelve hours of running have been added at the second highest Q^2 point. We allow 8 hours for energy changes, 8 hours for each angle change (which involves re-positioning BigBite and HCal), 36 hours to change to elastic calibration (which involves rigging out BigBite and moving the HRS-right to the desired angle), and half an hour for each of the small changes in HRS angle used for elastic calibration. The elastic calibration at the second Q^2 point has been eliminated. For efficiency, the two elastic calibration measurements will be run contiguously at the end of the run.

6 Comparison with Other Experiments

Fig. 1 compares the kinematic coverage and predicted errors of this measurement with those of the CLAS12 experiment [15]. The CLAS12 points are plotted at the scaled-dipole value used in the proposal as it is not clear how the systematic errors would scale with assumed form factor. Another relevant point for comparison of the two experiments is in the statistics of coincidence events which each will acquire. Since the statistics are limited by the neutrons, the counts of neutron-coincidences are compared in Fig. 7. The smaller acceptance of the present experiment is seen to be overcome by the fact that it runs at several thousand times higher luminosity. The statistics are seen to be significantly higher for the present measurement. This can be particularly advantageous at high Q^2. As mentioned previously, this allows the option of setting tighter cuts to improve systematic errors at the expense of statistics in the final data sample and to sub-divide the Q^2 range of each measurement into separate points. Perhaps more importantly it provides sufficient statistics to study and understand systematic effects. A well-defined quasi-elastic peak in $\theta_{pq} - W^2$ space will permit a more careful study of inelastic contamination, for example, than would be possible with an enhancement of only a few hundred events.

The running time for CLAS12 is 56 days while the present experiment requests 31 days. The total beam hours at the corresponding kinematics are shown under some of the points in Fig. 7.

The experiments are complementary in that they use very different apparatus and somewhat different techniques. The

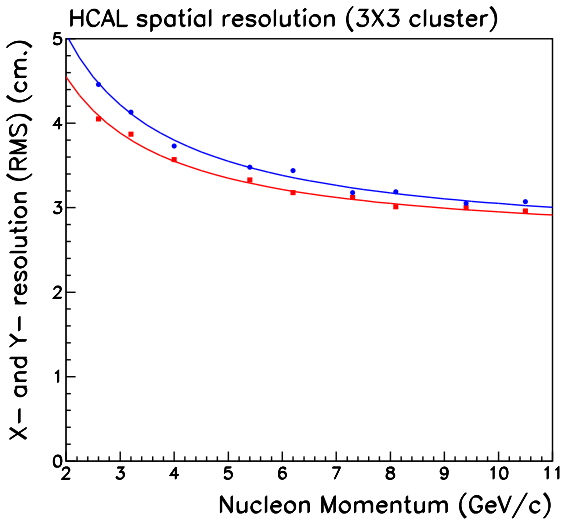

Figure 6: Predicted spatial resolution of neutrons (blue) and protons (red) found from Geant4 simulation [18, 19] of HCal. Each point represents one of the seven kinematic points of measurement. (Two proposed points at higher Q^2 are also shown.) Position is found as the $\sqrt{E}$-weighted mean position in a 3×3 array of blocks centered on the block with greatest energy-deposited.

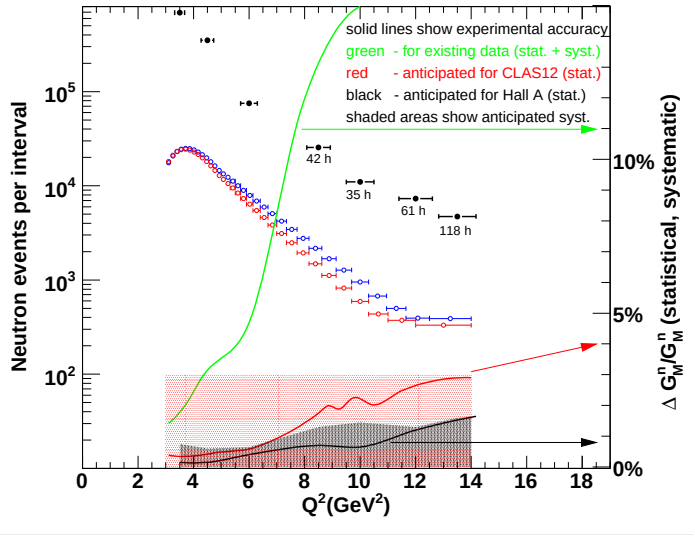

Figure 7: On a log scale (left axis), points compare expected number of detected coincidence neutrons within each kinematic bin for the present experiment (black) and for the CLAS12 experiment [4] (red for the Bodek parameterization, blue for a parameterizations using Kelly [6] for the proton and Alberico [7] for the neutron). On the right axis the solid curves show the present fractional uncertainty on G_M^n (green) and the statistical errors expected for CLAS12 (red) and the present experiment (black). The shaded areas show the anticipated systematic errors for the present experiment (gray) and CLAS12 (pink). (The CLAS12 proposal predicts constant 3% systematic errors.)

large acceptance of the CLAS12 detector provides several very useful features, such as easy calibration of the neutron detector efficiency (important at very low Q^2) and additional suppression of the inelastic events via the hermeticity cut. For experiments seeking such high precision in an essentially previously-unmeasured regime, it will be very valuable to compare results as a probe for unsuspected systematic errors.

7 Technical Progress Toward Realizing the Experiment

The complete account of progress on the Super BigBite project is presented in the update for E12-07-109 experiment. Here we list only items of special interest to the present experiment.

Collaboration and coordination This experiment is a part of three form-factor experiments which will use the Super BigBite apparatus. Carnegie Melon University is leading collaboration efforts on the hadron calorimeter. Rutgers University is leading collaboration efforts on trigger electronics.

Calorimeters Collaboration with the Dubna group (Prof. I. Savin) was organized for the design and construction of the hadron calorimeter. A Monte Carlo simulation of the HCal calorimeter was performed for a few GeV protons, neutrons,

and pions. The Monte Carlo simulation was also used to find the counting rate of the detector by using the DINREG event generator [20].

Trigger configuration A Flash ADC was developed by the JLab electronics group. It has been used successfully for the Gas Cherenkov counter of the BigBite spectrometer and currently in the detector of the Möller polarimeter. We plan to implement 16 such FADCs in the readout of the hadron calorimeter. A detailed design of the trigger logic based on the FADC and FPGA logic has been developed [12].

References

[1] S. Rock *et. al.*, Phys. Rev. D **46** 24 (1992).

[2] L. Durand, Phys. Rev.**115**, 1020 (1959).

[3] J Lachniet et al.,, Phys. Rev. Lett. **102**, 192001 (2009) JLab Experiment E-94-071
"The Neutron Magnetic Form Factor from Precision Measurements of the Ratio of Quasielastic Electron-Neutron to Electron-Proton Scattering in Deuterium", W. Brooks and M. Vineyard spokespersons.

[4] E12-07-104 proposal, "Measurement of the Neutron Magnetic Form Factor at High Q2 Using the Ratio Method on Deuterium", W. Brooks, G. Gilfoyle, K. Hafidi, and M. Vineyard spokespersons.

[5] A. Bodek et al., Jour. of Phys. **110** 082004 (2008).

[6] J.J. Kelly Phys. Rev. C **70**, 068202 (2004).

[7] W.M. Alberico et al., Phys. Rev. C **79**, 065204 (2009).

[8] `http://www.jlab.org/~bogdanw/gep_u.pdf`

[9] C.D. Roberts *et al.*, Eur. Phys. J. **ST 140**, 53-116 (2007);
I.C. Cloët *et al.*, Few-Body Systems **46**, 1-36 (2009).

[10] C.D. Roberts, private communication (2008).

[11] The Super-BigBite Spectrometer (SBS) Conceptual Design Report and SBS Technical Review Report can be found in `http://hallaweb.jlab.org/12GeV/SuperBigBite/SBS-CDR/`

[12] K. de Jager, G. Cates, B. Wojtsekhowski *et al.*, Electromagnetic Form Factors of the Nucleon using the 12-GeV CEBAF, `http://www.jlab.org/~bogdanw/EMFF.pdf`

[13] G. Cates, N. Liyanage, and B. Wojtsekhowski *et al.*, Jefferson Lab experiment E02-013.

[14] N.V. Vlasov et al., Inst. and Expt. Techniques **49** 41 (2006).

[15] G. Gilfoyle, private communication.

[16] A. Lung *et al.*, Phys. Rev. Lett. **70**, 718 (1993).

[17] J, Lachniet thesis, Carnegie Mellon University, unpublished, June, 2005
http://www-meg.phys.cmu.edu/ bquinn/jeff_thesis.pdf

[18] John Annand, private communication

[19] Fatiha Benmokhtar,private communication

[20] P.V. Degtyarenko, M.V. Kossov, H-P. Wellisch, Chiral Invariant Phase Space Event Generator, *Eur. Phys. J.* **A 8**, p. 217 (2000).

Table 4: Beam Time Request (beam hours). "Normal $\mathcal{L}$" refers to running at the standard luminosity given in Table 1. Reduced luminosity running is indicated as "Half $\mathcal{L}$" or "10% $\mathcal{L}$".

Q^2 (GeV/c)^2	3.5	4.5	6.0	8.5	10.	12.	13.5	
E (GeV)	4.4	4.4	4.4	6.6	8.8	8.8	8.8	
θ_e	32.5°	41.9°	64.3°	46.5°	33.3°	44.2°	58.5°	
θ_N	31.1°	24.7°	15.6°	16.1°	17.9°	13.3°		
d(e,e')								
Normal $\mathcal{L}$	12	12	18	18	24	48	96	
Dummy target	2	2	2	2	3	4	8	
Half $\mathcal{L}$	12	12	12	12				
Dummy half $\mathcal{L}$	2	2	2	2				
10% $\mathcal{L}$	12	12						
Dummy 10% $\mathcal{L}$	2	2						
H(e,e')								
Normal $\mathcal{L}$	3	3	24	4	4	4	5	
Half $\mathcal{L}$	3	6	2	2	2	2	2	
10% $\mathcal{L}$	18	18						
BigBen off	6	6	6	2	2	3	6	
Dummy target	2	2	2					
H(γ,π^+)								
Radiator	24		12					
Dummy target	2		2					
No radiator	6		3					
Total	106	74	89	42	35	61	118	$\Rightarrow$ 525
Commissioning								96
3 Energy changes								24
7 BigBite/HCal angle changes								56
Rig out BigBite/move HRS								36
4 small HRS moves								2
Beam request								739 $\approx$31 days